



Published in final edited form as:

Curr Protoc Neurosci. 2010 January ; 0 2: Unit2.1. doi:10.1002/0471142301.ns0201s50.

Fluorescence Microscopy: A Concise Guide to Current Imaging Methods

Christian A. Combs

NHLBI Light Microscopy Facility, NIH, Building 10, Room 6N-309, 10 Center Dr. Bethesda, MD 20892, Phone: 301-496-3236, Fax: 301-480-1477, combsc@nhlbi.nih.gov

Keywords

review; confocal; two-photon; structured light; and STED

Introduction

Fluorescence microscopy is a powerful tool for modern cell and molecular biologists and, in particular, neurobiologists. It provides a window into the physiology of living cells at sub-cellular levels of resolution. This allows direct visualization of the inner workings of physiological processes at a systems level context in a living cell or tissue. Fluorescence microscopy enables the study of diverse processes including protein location and associations, motility, and other phenomenon such as ion transport and metabolism. This versatility explains why thousands of papers a year are published using variants of fluorescent microscopy techniques. Many new techniques have been developed over the last decade which enable more comprehensive exploitation of light for biologic imaging. These advances include the wide-spread use of fluorescent proteins (for review see (Shaner et al., 2005), the myriad number of new fluorophores available (for reviews see (Eisenstein, 2006; Suzuki et al., 2007), the growth of the utility of the basic confocal microscope, the use of multi-photon microscopy to optically image far deeper into tissues, and the breaking of the diffraction limit for “super-resolution”. Many of the new advanced techniques are now being commercialized, opening their use to a large fraction of modern biologists. However, for the biologist inexperienced in light microscopy, matching the best technique to the biological experiment can prove to be difficult. Optimal use of fluorescence microscopy requires a basic understanding of the strengths and weaknesses of the various techniques as well an understanding of the fundamental trade-offs of the variables associated with fluorescent light collection.

In a very simple form, the ideal light microscopy experiment can be viewed as optimizing the competing properties of image resolution (in the XY or lateral direction as well as the Z or axial dimension), imaging speed (and/or acquisition time), and the amount of signal collected from the fluorescing sample (Figure 1). This is bounded by the limits imposed by photo-bleaching and/or photo-toxicity. In many experiments, light levels at the diffraction limited spot (focused by the objective) can be very high. This can lead to destruction of the fluorophore and unwanted biological consequences leading to cell death or changes in the physiology of the cells or tissue being illuminated. Given these constraints, these variables are difficult to balance and require careful attention to detail and systematic empirical testing. On top of these basic variables other secondary variables also can become important such as the cost of the necessary equipment and the difficulty of the technique.

This review is intended to expand and build-upon the last review of fluorescence microscopy in this series (Coling and Kachar, 1997) which provided a foundation for

understanding fluorescence microscopy and the basics of immuno-labelling. In this review, knowledge of the basics of fluorescence microscopy (including wide-field microscopy) presented in that paper will be assumed. The object of this review is to provide non-expert microscopists a concise description and guide to select techniques that may have the widest appeal and that are, or will soon be, commonly used in most light microscopy core facilities or advanced biological research labs. The techniques to be reviewed encompass the most basic (such as wide-field fluorescence microscopy) to cutting edge techniques like Stimulated Emission Depletion (STED) microscopy. An emphasis will be placed on explaining the strengths and weaknesses of these techniques in terms of balancing the variables discussed in Figure 1. A table at the end of this review will summarize this discussion and should serve as a quick guide for choosing the appropriate imaging modality from among the techniques discussed.

Wide-field Fluorescence Microscopy (WFFM) Techniques

In the most basic form (WFFM) involves exciting the fluorophore(s) in the sample of interest using a fluorescence light source, a microscope, excitation and emission filters, and an objective. The resulting emission light, of longer wavelength, is observed through the microscope eyepieces or by a camera followed by computer digitization (for reviews see (Coling and Kachar, 1997; Inoue and Spring, 1997). Over the last decade developments in microscope and camera design, light filters, and in new techniques have greatly improved resolution and light collection for WFFM.

One of the most significant advancements has been the development of electron multiplied (EMCCD) and very low-noise, cooled CCD cameras. These cameras allow for fast detection of low-light fluorescence (EMCCD) or allow for the gradual accumulation of fluorescence signal to be integrated with little noise (cooled CCD) while still maintaining high resolution. These advancements allow for faster imaging and better contrast at low signal levels such as when the excitation light is purposefully minimized to prevent photo-bleaching or photo-toxicity.

In addition to cameras, wide-field microscopy has also been improved by better light filters, mirrors, and objectives. Commercially available filters, for instance from Chroma Inc (Rockingham, VT), (Omega Brattleboro, VT), or Semrock (Rochester, NY), have very high transmittance or reflection values enabled through new sputter-coating technologies. Also, these filters can have very sharp wavelength dependencies which enable multi-color discrimination. In the last decade, all of the major microscope companies (such as Leica, Nikon, Olympus, and Zeiss) have also improved microscope objectives. These new objectives have very flat fields (which decreases objective induced gradients in intensity across an image), long working distances with good resolving power, improved light transmission from the near UV to the infra-red, and are available in varieties that match the refractive index of the sample being imaged.

The main advantages of basic WFFM are that it is the least expensive technique, it provides good XY dimension resolution (the ability to distinguish fine detail in a specimen in the XY dimension), can provide very fast temporal resolution (particularly with the new EMCCD cameras), and in many cases requires the least amount of excitation light (Table 1). XY resolution (R_{xy}) in wide-field microscopy is a function of the NA of the objective and the wavelength of the excitation light according to Ernst Abbe's diffraction limit expression:

$$R_{xy} \approx 0.61\lambda / NA$$

Where λ is the wavelength of the emission light, NA is the numerical aperture of the objective. For a high NA objective (NA 1.4) lens this limit is around 200nm. All of the techniques listed in Table 1 are approximately limited to this type of XY resolution except where super-resolution is indicated. The main disadvantage of basic WFFM is that all of the emission light is integrated through the sample in the Z dimension. Therefore, it is difficult to tell where the fluorescence from a point in the sample originated in the Z-dimension. For samples that are thin or where Z-discrimination is not critical this may not be a limiting factor. For thick samples (such as live cells or tissues) where optical sectioning is critical or where out of focus light obscures details even in the XY plane, other techniques such as confocal or multi-photon microscopy may be more appropriate (see the following sections), although fluorescence deconvolution microscopy and structured light microscopy (SLM) are WFFM techniques that are commercially available.

Structured Light Microscopy (SLM) is a form of WFFM that enables optical sectioning. SLM works by inserting a moveable grid pattern into the optical path of the excitation light in the wide-field microscope. This produces a pattern in the images produced. The pattern is moved in the XY and even Z-dimension and the way that the detected fluorescence from the sample interacts with the pattern is then analyzed using a simple mathematical formula to create the optical sections (Figure 2). Many commercial systems are available for SLM and also moveable grating patterns are available for those wishing to modify existing WFFM microscopes. In the last few years SLM has been shown capable of producing super-resolution images (\approx half the diffraction limit) (Gustafsson, 2000; Schermelleh et al., 2008).

The main advantage of SLM is that one can optically section using WFFM without the cost of expensive confocal systems and in some cases produce super-resolution images without the cost or technical complexity associated with other super resolution techniques such as Stimulated Emission Depletion Microscope (STED, discussed in a section later in the paper). The main disadvantage of this technique is that multiple images must be taken to provide optical sections. This can lead to photo-bleaching. Also the optical sectioning ability of SLM is negated if the sample moves while the different images are being captured (as would be the case in live cells).

Deconvolution fluorescence microscopy (DFM) is a form of WFFM. DFM requires prior knowledge of the point spread function (PSF, for more information on the PSF see (Coling and Kachar, 1997)) to allow optical sectioning. In this technique, multiple XY sections are imaged through the sample in the Z-dimension. The resulting stack of images, still lacking Z-dimension discrimination, are then analyzed using an empirical or idealized mathematical model of the PSF created by the microscope optics. This analysis results in a volumetric recreation of the sample in 3D space. DFM can also be used to enhance other techniques that are able to optically section such as confocal and two-photon microscopy (discussed below). Software for DFM is available commercially or through plug-ins for the free image analysis program ImageJ (<http://rsbweb.nih.gov/ij/>, NIH, Bethesda, MD). Although DFM is a powerful technique when used in capable hands (reviews include (Boccacci and Bertero, 2002; Wallace et al., 2001)), the novice user should be warned that optical sectioning is done indirectly using a mathematical model. Knowledge of the limitations of the model used for DFM is critical to understanding the images produced and interpretation of the data. Given these constraints it is beyond the scope of this paper and is not listed in Table 1.

Modern Confocal Microscopy

The laser scanning confocal microscope (LSCM) remains a key piece of equipment in most imaging laboratories. Most modern LSCM systems offer a variety of advantages and are equipped with software to perform complex 3D (z-stack), 4D (z-stack over time), or even

5D (z-stack over time including spectral imaging) experiments. These microscopes often include software to facilitate data acquisition for complex methodologies such as spectral deconvolution, Fluorescence Recovery After Photobleaching (FRAP), and Fluorescence Resonance Energy Transfer (FRET). There have been many reviews written about confocal microscopy, but readers are encouraged to see the following texts for comprehensive information regarding all forms of confocal microscopy (as well as other microscopy techniques)(Hibbs, 2004; Pawley, 2006).

In the last few years, many changes have been made to improve these microscopes, but the fundamental design for optical sectioning remains largely unchanged. Figure 3 shows a simplified diagram of the light path of an LSCM. This figure shows that laser light is directed to the sample through collimating and beam steering optics, scanning mirrors (which sweep the laser beam over the field of view) and an objective that focuses the light to a diffraction limited spot in the sample. Emission light from the sample is directed to light sensing detector(s) (typically photomultiplier tubes, also known as PMT's) through a pinhole that is in the conjugate image plane to the point of focus in the sample. After spatial filtering by the pinhole, the light is sensed by the detectors, and a proportionate voltage is produced and amplified and converted into digital levels for image display and storage.

At the heart of the confocal microscope is the pinhole. When placed in the conjugate image plane to the point of focus on the sample it enables optical sectioning (Figure 3). The pinhole optically sections by acting as a barrier to light originating from other focal planes in the sample. Although the pinhole facilitates optical sectioning it must be understood that the axial resolution is still worse than the XY resolution (which is similar to WFFM). Axial resolution (R_z) in the confocal microscope is set by the expression:

$$R_z = 1.4\lambda n / (NA)^2$$

where λ is the wavelength of the emission light, n is the refractive index of the mounting medium, and NA is the numerical aperture of the objective. At an intermediate emission wavelength when coupled with a pinhole and a high numerical aperture lens this would enable an ideal axial resolution of approximately 0.6 μm . In practical terms, axial resolution is likely to be between 0.6 and 1.0 μm . The difference between the XY and Z dimensions leads to a resolution limit that is ellipsoidal in shape in 3D space.

Most LSCM manufacturers also offer a spectral imaging option that will allow for either variable band-pass emission filtering or spectral detection on a per pixel basis. This works by placing either a diffraction grating or a prism in the light path before the PMT detector(s). In many cases, polychromatic (spectral) light is passed to a PMT array to detect a range of wavelengths either sequentially or simultaneously depending on the range of wavelengths desired. Although this option allows for more versatility and direct selection of the emission range it can come at the cost of less sensitive detection, due to the light loss in the additional optics required and in the spreading out of the light over a series of detectors to enable the spectral detection.

Table 1 shows the main advantages and disadvantages of LSCM. The main advantage of LSCM is that one may optically section while still doing complex experiments. Another advantage is the versatility of imaging capabilities and types of experiments one can perform. Most of these systems have multiple channels for multi-color, variable pinhole sizing for selecting the desired optical section thickness (usually sacrificing z-resolution for signal intensity), and software for variable ROI (region of interest) selection. Another

example would be the ability to separate spectrally overlapping fluorescent proteins with spectral detection and spectral deconvolution methods. In addition, these systems, particularly in the inverted microscope configuration, can accommodate both live cells or fixed cells or tissue. Many manufacturers also provide options for small stage incubation systems. These systems allow long term experiments, particularly when coupled to automated acquisition software that enables auto-focusing algorithms in tandem with precise XYZ stage movement. Disadvantages of a modern LSCM system include the relatively low scan speed (as the beam must be swept through each pixel in the field of view), the relative price, and the amount of light impinging on the sample. The flexibility of the LSCM does mitigate many of the disadvantages, and in many instances, one can balance the imaging conditions among the variables listed in figure 1 to get the most out of a given experiment. For instance, if full-frame imaging speed is too slow to capture a physiological event in a live cell experiment one might use a small ROI to increase temporal resolution. Despite this flexibility, one concern always remains and should be considered when conducting LSCM and that is keeping the light levels low enough to avoid killing or bleaching the sample.

Another type of confocal microscopy is multipoint confocal microscopy, which includes Nipkow spinning disk, swept-field, and slit line scanning microscope systems. Each of these types of microscope systems shares the characteristic that multiple parts of the sample are imaged at once, thus increasing imaging speed. In the case of the Nipkow spinning disk and swept field systems, a sensitive camera (typically an EMCCD) is also employed. This allows for fast (usually tens to hundreds of milliseconds vs. the seconds timeframe of the LSCM), relatively low-light confocal imaging. Nipkow scanning systems have a drawback in that confocal sectioning can only occur with relatively high NA objective lenses and the pinhole size is fixed. In the case of the slit-scanning confocal microscopes, there is also a modest decrease in resolution for the X or Y dimension. All of these systems are usually less expensive than a LSCM system but can become relatively expensive if a very sensitive camera is also included.

Total Internal Reflection Fluorescence (TIRF) Microscopy

TIRF microscopy provides very good axial resolution (Z-direction, along the axis of illumination) to levels of approximately 200nm (for review see (Toomre and Manstein, 2001). Not only is the axial resolution better than most other techniques but this also can greatly reduce background light (thus increasing the signal to noise ratio) that can obscure fine details. The setup for TIRF microscopy is very simple and is similar to wide-field microscopy except that it employs an oblique angle for the excitation light impinging on the sample. When the incidence angle is set to a critical angle relative to the coverslip, the excitation light is totally internally reflected (Figure 5A). This generates an electromagnetic field at the interface, called an evanescent wave, which excites fluorophores in nearly the same manner as conventional fluorescence excitation light. The key here is that the evanescent wave propagates only a short distance above the coverslip (Figure 5B). Therefore, only fluorescent molecules in close proximity to the coverslip are excited. Figure 5C shows a wide-field and a TIRF image of the fluorescence from EGFP labeled myosin in drosophila embryo hemocytes. As can be seen in the overlay, only myosin molecules in portions of the cell near the coverslip are excited, showing where the cell is closest to or touching the coverslip.

As mentioned above, the decay of the evanescent wave is exponential to the distance above the coverslip. This relationship can be expressed as:

$$I(z) = I(o)e^{-z/d}$$

Where $I(z)$ represents the intensity at a given distance (z) from the coverslip, $I(o)$ is the intensity at the coverslip, and d is the penetration depth. The penetration depth d decreases as the reflection angle (θ_c , shown in Figure 5) of the incident beam grows larger. This value is also dependent on the illumination wavelength and on the refractive index of the media present at the interface. In a typical commercially available objective-based TIRF system, the reflection angle of the excitation light can be changed mechanically on a special illumination module attached to the epi-fluorescence port of a wide-field microscope. Turning of the micrometer changes the position of the beam traveling in the periphery of the objective back aperture, resulting in a change in the angle of the beam exiting the front element. Another requirement for the typical objective based TIRF system is that high numerical oil objectives (>1.4 NA) are required to generate the necessary reflection angles to establish the evanescent wave.

As is shown in Table 1, the main advantage of TIRF is enhanced z -resolution. XY resolution benefits from a reduction in background fluorescence. Also, relative to other techniques such as confocal and two-photon, a commercial turn-key objective based TIRF microscope system is inexpensive. These systems only require a microscope, special illuminator(s), lasers, camera, and a high numerical aperture objective lens. The main disadvantage of TIRF is related to its main advantage in that only fluorophores in the first 200-300nm can be excited. This obviously limits imaging to near the coverslip but enable a z -resolution to the same depth as the penetration of the evanescent wave. Also, because the intensity of the evanescent wave decreases according to this relationship, fluorescence intensity will be a function of distance from the coverslip as well as the concentration of the fluorescent molecules. This makes quantification of depth from the coverslip or comparisons of molecular concentration difficult from TIRF images.

Two-Photon Fluorescence Microscopy (TPFM)

TPFM is a type of laser scanning microscopy that is particularly useful for imaging thick samples both *in vitro* and *in vivo*. It has been used to image hundred's of microns into tissues (for reviews see (Diaspro et al., 2006; Svoboda and Yasuda, 2006)). An example of this type of imaging is shown in figure 6C. Deep imaging is achieved by using pulsed near-infrared excitation light. Infrared light penetrates much deeper into tissue do to decreased scattering and absorption than the visible wavelengths used in standard confocal and wide-field microscopy. This technique is also good for limiting the excitation (and often photo-bleaching and possible photo-toxicity) to just one focal plane. This also has the added benefit of eliminating the need for a pinhole aperture for optical section as is used in confocal microscopy. In confocal microscopy the pinhole is used to reject out-of-focus emission light from reaching the photo-sensor (photo-multiplier tube or camera). In effect, the pinhole selects only a small portion of the emission light to achieve optical sectioning with much of the emission light “thrown away”. In TPFM it is the excitation pulse that provides the optical sectioning; therefore all of the light can be collected from the excited focal spot and none of the scattered or ballistic emission light photons need be wasted during collection. TPFM is a form of multi-photon imaging. Multi-photon imaging refers to techniques where more than one photon at a time is used to excite a fluorophore (other examples are Second Harmonic Generation (SHG) imaging and Coherent Anti-stokes Raman (CARS) microscopy. CARS and SHG are not fluorescence techniques and are outside the scope of this review).

TPFM excitation is generated when a fluorophore absorbs two photons essentially simultaneously. This roughly doubles the amount of energy absorbed by the fluorescent molecules which drives their excited electrons to the same energy level as would the absorption of one photon at one-half the two-photon excitation wavelength (Fig. 6A). An example would be the excitation of GFP (typically excited around 488nm in a confocal experiment) at around 960nm using a pulsed laser. This is an oversimplification, as the actual TPFM absorption spectra for many fluorophores are over 100nm broad, and “selection rules” that govern the relative strengths of absorption bands vary between one-photon and two-photon excitation, but in most cases that is a good starting point for guessing where the maximal TPFM excitation occurs. The broad spectral absorption range of the typical two-photon fluorophore allows for multiple fluorophores in a sample to be excited at one wavelength simultaneously. Corresponding emission wavelengths for each fluorophore are then separated in different channels with the appropriate set of dichroic and emission filters or with spectral detection. The inherent optical sectioning ability of two-photon excitation occurs due to increased probability of two-photon absorption that occurs at the diffraction limited spot due to spatial energy crowding (Figure 6B). This can be seen in the equation for time averaged two-photon fluorescence intensity (I_f):

$$I_f \approx \delta_2 \eta (P_{ave}^2 / \tau_p f_p) (NA^2 / hc \lambda_{exc})^2$$

Where δ_2 is the two photon cross section for the fluorophore, η is the quantum yield of the fluorophore, P is the intensity (power) of the excitation light, τ_p is the pulse width of the excitation pulses, f_p is the repetition rate of the laser, NA is the numerical aperture of the objective, h and c are Planck's constant and the speed of light respectively, and λ_{exc} is the wavelength of the excitation light (Diaspro et al., 2006). In fact, the probability of two-photon absorption decreases as the fourth power of distance away from this focal region along the z-axis (NA dependence) and increases as the square of the intensity (mW of power are typically required). Another variable is the temporal pulse width, τ_p , of the excitation light pulse as it reaches the sample. In general, short pulse widths (on the order of 100fs) are optimal for two-photon excitation.

Commercially available turn-key confocal systems usually consist of a modified point-scanning confocal microscope which includes a Ti:Sapphire pulsed laser (often automatically tunable over a broad range of wavelengths) and non-descanned detector channel(s). The non-descanned detector is a PMT mounted closer to the sample where the emission does not travel back through the scan-head. Since no pinhole is necessary, this configuration can be employed to reduce light losses that would occur if the emission light passed back through the scan-head. Typically, commercially available pulsed lasers produce approximately 100fs pulses at rate of 80MHz. Dispersion in the optics of the microscope and objective will lengthen these pulse widths by at least a factor of two. Recently, commercial lasers optionally include an additional unit for pre-compensation of this dispersion which can reduce the pulse length at the sample (which restores the two-photon fluorescence efficiency).

In summary, as is shown in table 1, the main advantage of TPFM is the depth of imaging (hundreds of microns) into the sample. Another important advantage is that the bleaching and phototoxicity are limited to the focal plane, however in the focal plane the damage can be greater due to the higher light intensities (mW compared to μ W in confocal) needed for TPFM. TPFM typically requires the same time frame for acquisition as traditional CLSM (on the order of 1s/frame). One big disadvantage is cost due to the need for a point-scanning microscope and a tunable pulsed Ti:Sapphire laser. This cost increases substantially if one

also adds a pre-compensation unit to correct dispersion in excitation pulse lengths or selects higher power lasers whose gain enables lasing at the hard to tune to regions approaching 700nm or somewhat above 1000nm.

Stimulated Emission Depletion (STED) Fluorescence Microscopy

STED microscopy, developed by Stefan Hell and colleagues, is a relatively new super-resolution technique that has been shown to improve fluorescence microscopy resolution by approximately an order of magnitude over traditional diffraction limited techniques such as LSCM. STED can produce optical resolution to levels that were previously thought possible only with electron microscopy, and it has been used to examine key biological processes that no other technique could have examined (Kellner et al., 2007; Willig et al., 2006b). STED improves resolution by a direct reduction in the emission spot size by using a second laser beam (the STED beam) (Figure 7 and explained below). It is important to note that the improvement in resolution is done directly without the need for post processing and mathematical redistribution of the light, as is done in deconvolution microscopy or by combining multiple images that has taken with respect to a moveable grid pattern, as is done in structured light microscopy. STED is so straight-forward that to the user this seems like a normal point-scanning technique such as LSCM or TPFM. In fact, Leica Microsystems (Wetzlar, Germany) has now commercialized this system on their current point-scanning microscope stand.

Figure 7A shows the setup for the STED technique. In the commercially available system (Leica Microsystems), two pulsed (picosecond time-domain) lasers are included. One excites the fluorophore as would normally occur in a LSCM experiment. The second, longer wavelength laser is used for the patterned quenching of the focal spot (STED beam). Specialized optics in the scanhead spatially shapes the phase of the STED beam wave-front to form a doughnut pattern (with a sharply decreased laser intensity at the central portion of the doughnut) at the focal spot. The STED wavelength must be red shifted (longer wavelength) such that it does not overlap the absorption spectrum of the fluorophore but does overlap with its emission spectrum. In this way, it quenches (forces the excited electrons into a lower energy state without giving off fluorescent light) the emission of the fluorophore in the area of the spot where the STED beam overlaps the excitation beam. This reduces the ultimate emitting region to that of the middle of the doughnut. The size of this region is related to the power of the STED beam according to the following equation:

$$R \approx \lambda / (2NA(1+\zeta)^{0.5})$$

where R is the lateral (XY) resolution, λ is the wavelength of the excitation light, NA is the numerical aperture of the objective, and ζ describes the intensity of the STED beam. Stefan Hell and colleagues have reported limiting the excitation size to around 30nm, or almost the size of a few fluorescent molecules (Willig et al., 2007).

The main disadvantages of the STED approach are the cost of the system and the amount of power that impinges on the sample (Table 1). The cost of the system is relatively high because two pulsed lasers are needed in addition to the already expensive laser scanning microscope system and very sensitive emission detectors (avalanche photo-diodes) required (fast electronics and are sensitive in the far-red portion of the emission spectrum). Another disadvantage is the amount of power that is used for a STED system is high (tens of mW for the second beam). Since there is the potential for destruction of the probe or sample, only very photo-stable probes can be used. The list of probes that have been used to date are

LDS721, certain ATTO dyes (AttoTech), and fluorescent proteins (Willig et al., 2006a). While the current commercial system can only improve lateral resolution, axial resolution can also be improved (Hell, 2007). It remains unclear how deep into tissue this technique remains effective. It is likely that the loss of coherence of the shape of the STED beam with depth is a limiting factor and will be tissue dependant. In general, STED is most effective for fixed tissue as movement or diffusion of the fluorescent marker during scanned imaging will negate any gains in resolution.

Final Considerations

Many of the microscope systems available from manufacturers have become very easy to run. While this provides easy image acquisition for many of the techniques listed in Table 1, the danger remains that an incomplete understanding of the fundamental physics and limitations of the techniques can result in wrong, incomplete, or biased data (as recently noted in (Pearson, 2007)). It should be noted that Table 1 is only a rough guide to the commercially available fluorescence microscopy techniques and the reader should consult other sources to provide more complete understanding. There are many reviews available that are not listed here and many good web based resources such as *Molecular Expressions: Exploring the World of Optics and Microscopy* (<http://www.microscopy.fsu.edu/>), *The Molecular Probes Handbook* (<http://probes.invitrogen.com/handbook/>) and the *Confocal Listserv* (<http://listserv.acsu.buffalo.edu/cgi-bin/wa?A0=CONFOCAL&D=0&F=P&T=0>). One final note is that one must also be able to analyze the data one has collected. There are many good commercially available image processing software packages available as well as the comprehensive free program ImageJ (<http://rsbweb.nih.gov/ij/>). Last, the mention of any company producing microscopy related products in this work is in no way intended as an endorsement of them by the National Institutes of Health or the author.

Acknowledgments

The author wishes to thank Dr. Jay Knutson, Dr. Paul Jobsis, and Dr. Aleksandr Smirnov for useful discussions and critical reading of this manuscript. The author also thanks Ethan Taylor and Alan Hoofring for help with many of the figures in this work. The author also thanks those who permitted reprinting of some of the figures in this article. Those authors are cited in the figure legends and permission was granted by the publishers. This work was supported by the intramural research program of the National Institutes of Health and the National Heart Lung and Blood Institute.

References

- Boccacci, P.; Bertero, M. Image-restoration methods: basics and algorithms. In: Diaspro, A., editor. *Confocal and Two-Photon Microscopy: Foundations, Applications, and Advances*. Wiley-Liss; New York: 2002. p. 253-269.
- Coling D, Kachar B. Theory and application of fluorescence microscopy. *Curr Protoc Neurosci*. 1997; Chapter 2:1. Unit 2.
- Diaspro A, et al. Multi-photon excitation microscopy. *Biomed Eng Online*. 2006; 5:36. [PubMed: 16756664]
- Eisenstein M. Helping cells to tell a colorful tale. *Nat Methods*. 2006; 3:647–655.
- Gustafsson MG. Surpassing the lateral resolution limit by a factor of two using structured illumination microscopy. *J Microsc*. 2000; 198:82–7. [PubMed: 10810003]
- Gustafsson MG. Nonlinear structured-illumination microscopy: wide-field fluorescence imaging with theoretically unlimited resolution. *Proc Natl Acad Sci U S A*. 2005; 102:13081–6. [PubMed: 16141335]
- Hell SW. Far-field optical nanoscopy. *Science*. 2007; 316:1153–8. [PubMed: 17525330]
- Helmchen F, Denk W. Deep tissue two-photon microscopy. *Nat Methods*. 2005; 2:932–40. [PubMed: 16299478]

- Hibbs, AR. Confocal Microscopy for Biologists. Springer; 2004.
- Inoue, S.; Spring, KR. Video Microscopy: The Fundamentals. Springer; 1997.
- Kellner RR, et al. Nanoscale organization of nicotinic acetylcholine receptors revealed by stimulated emission depletion microscopy. *Neuroscience*. 2007; 144:135–43. [PubMed: 17049171]
- Livet J, et al. Transgenic strategies for combinatorial expression of fluorescent proteins in the nervous system. *Nature*. 2007; 450:56–62. [PubMed: 17972876]
- Pawley, JB., editor. Handbook of Biological Confocal Microscopy. Springer; 2006.
- Pearson H. The good, the bad and the ugly. *Nature*. 2007; 447:138–40. [PubMed: 17495900]
- Schermelleh L, et al. Subdiffraction multicolor imaging of the nuclear periphery with 3D structured illumination microscopy. *Science*. 2008; 320:1332–6. [PubMed: 18535242]
- Shaner NC, et al. A guide to choosing fluorescent proteins. *Nat Methods*. 2005; 2:905–9. [PubMed: 16299475]
- Suzuki T, et al. Recent advances in fluorescent labeling techniques for fluorescence microscopy. *Acta Histochem Cytochem*. 2007; 40:131–7. [PubMed: 18224244]
- Svoboda K, Yasuda R. Principles of two-photon excitation microscopy and its applications to neuroscience. *Neuron*. 2006; 50:823–39. [PubMed: 16772166]
- Toomre D, Manstein DJ. Lighting up the cell surface with evanescent wave microscopy. *Trends Cell Biol*. 2001; 11:298–303. [PubMed: 11413041]
- Wallace W, et al. A workingperson's guide to deconvolution in light microscopy. *Biotechniques*. 2001; 31:1076–8. 1080, 1082 passim. [PubMed: 11730015]
- Willig KI, et al. STED microscopy with continuous wave beams. *Nat Methods*. 2007; 4:915–8. [PubMed: 17952088]
- Willig KI, et al. Nanoscale resolution in GFP-based microscopy. *Nat Methods*. 2006a; 3:721–3. [PubMed: 16896340]
- Willig KI, et al. STED microscopy reveals that synaptotagmin remains clustered after synaptic vesicle exocytosis. *Nature*. 2006b; 440:935–9. [PubMed: 16612384]

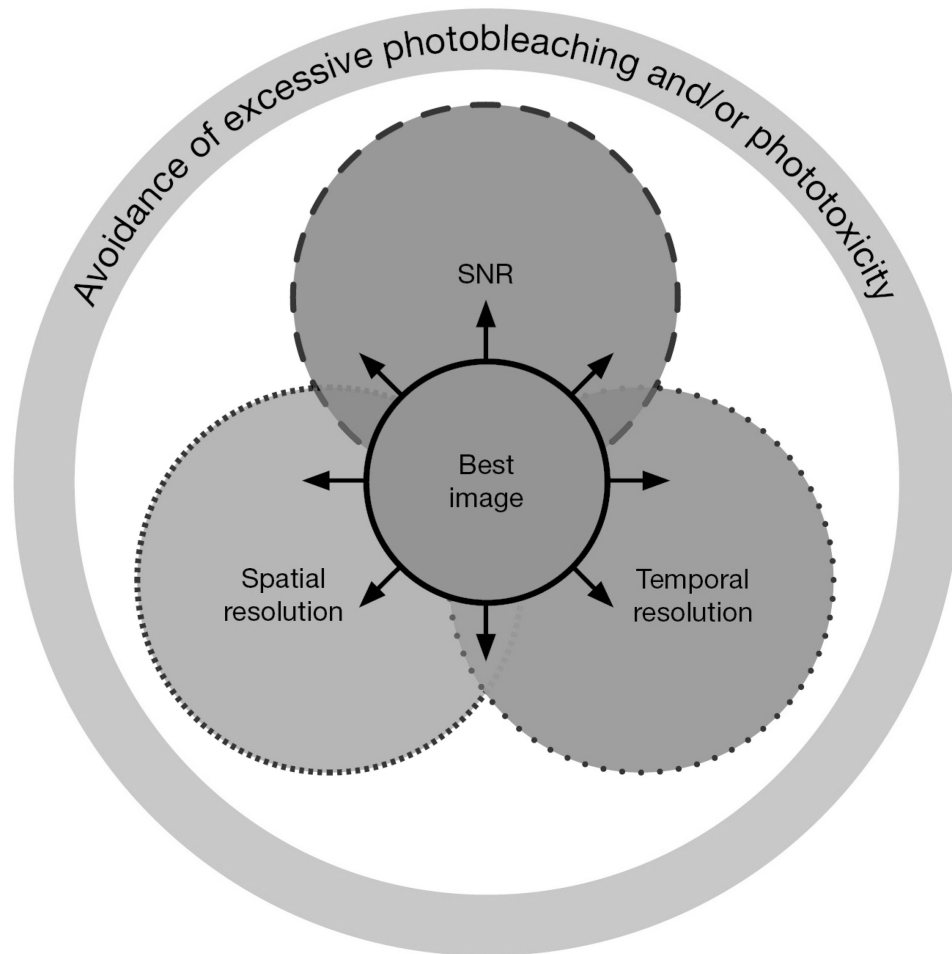


Figure 1.

Diagram of some of the critical opposing factors in an imaging experiment. The best image is one that can balance these factors to obtain the necessary information while avoiding photobleaching or phototoxic effects. Table 1 outlines how these factors differ between the various commercialized microscopy techniques discussed in this work.

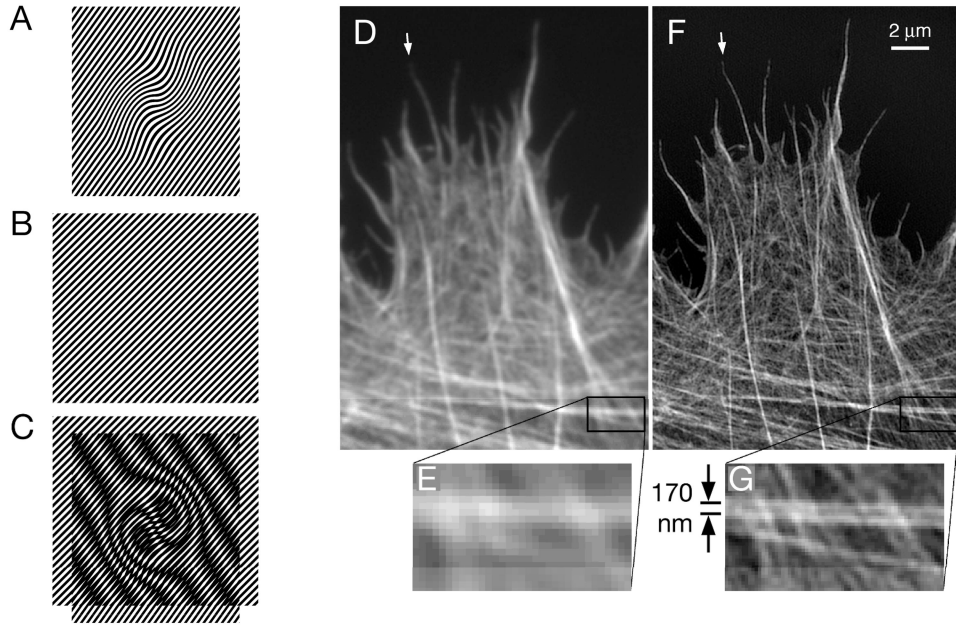


Figure 2.

The basic principles of structured light microscopy are shown in panels **A**, **B**, and **C**. If an unknown pattern (such as a biological sample) represented in (**A**) is multiplied by a known regular illumination pattern (**B**) then a beat pattern (moiré fringes) will appear (**C**). The pattern is the difference between the sample and the regular illumination pattern and is coarse enough to be seen through the microscope even if the original pattern in the sample was not resolvable. By moving the grid and the sample in space and computationally processing the resulting data an image can be generated that has resolution at least $2\times$ better than a conventional wide-field image. **D** and **F**. Confocal and structured light images respectively of the edge of a HeLa cell showing the actin cytoskeleton. **E** and **G** show enlargements of the images in **D** and **F**. The apparent fiber diameters are 110-120nm in the structured light images compared to 280 to 300nm in the confocal image. Figure **A**, **B**, and **C** are reproduced with permission from (Gustafsson, 2005). Figures **D** and **E** are reproduced with permission from (Gustafsson, 2000). Panels **A**-**E** were originally published in color and have been altered here to black and white.

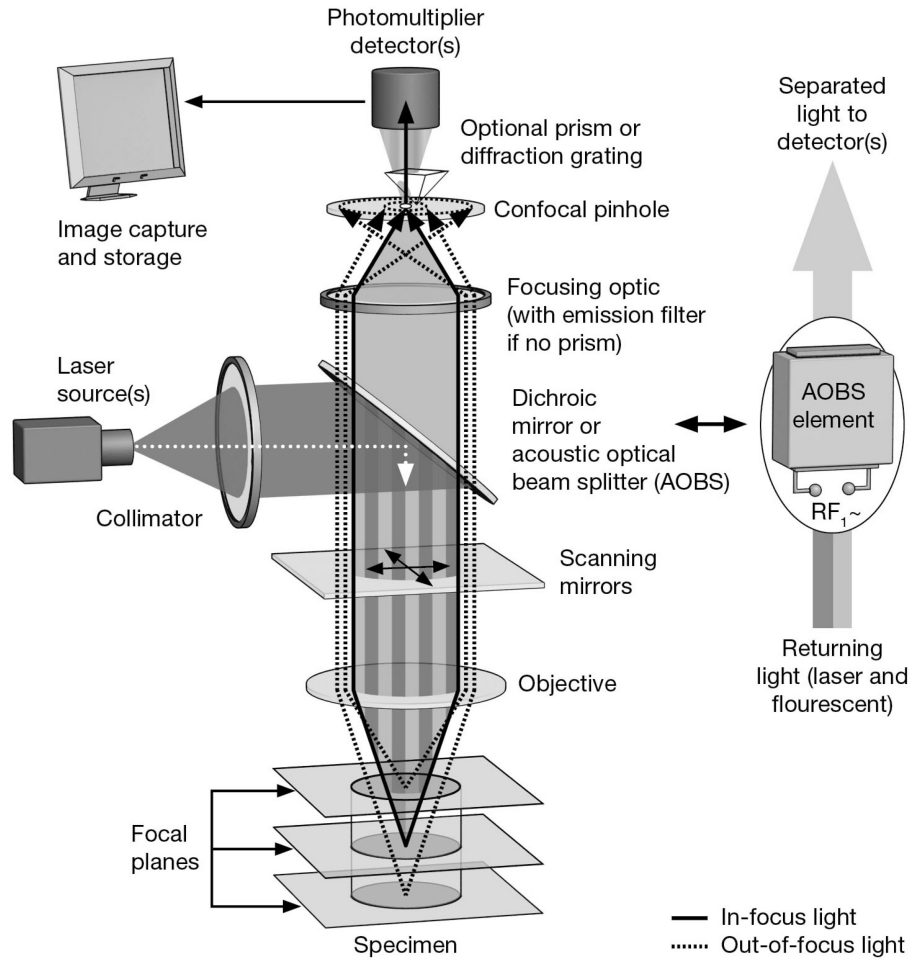
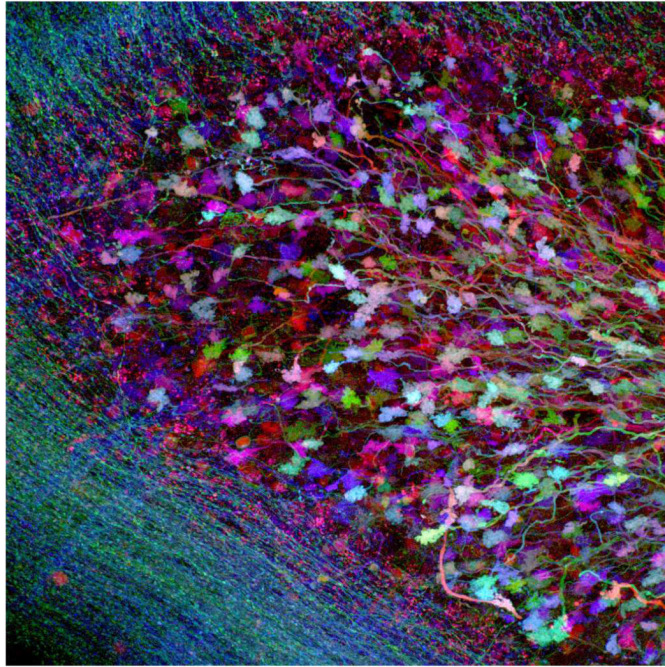


Figure 3.

Basic architecture of a modern confocal microscope. Excitation light from laser is passed through the various collimating optics in a scan-head to either a variable dichroic mirror (Nikon, Zeiss, or Olympus) or an AOBS (Acousto-Optical Beam Splitter) (Leica) where it is reflected through the objective and focused to a point on the sample. Moveable mirrors in the scan-head before the objective scan the excitation beam over the sample, a point at a time, to build the image. Fluorescence emission light passes back through the objective, through the dichroic or AOBS to the light sensing PMT(s) (photo-multiplier tube). An aperture (pinhole) placed in the conjugate image plane to the point of focus in the sample allows only light from the focal plane to impinge on the sample and out-of-focus light is blocked. The pinhole can be made larger to allow for larger optical sectioning capability allowing more out of focus light to impinge on the PMT(s). In some models a diffraction grating or prism placed in the beam-path of the emission light can act as a variable band-pass filter or as a spectral detector if the polychromatic light is spatially spread on a number of PMTs.

(Color)



(Black and White)

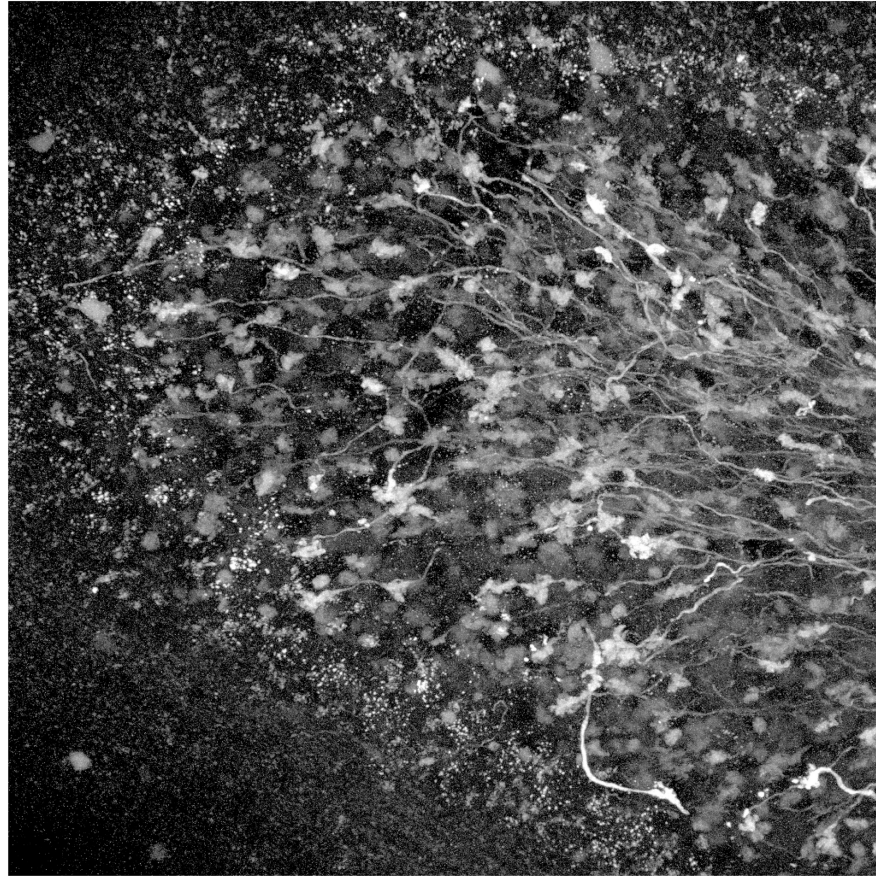


Figure 4. Maximum projection reconstruction from confocal images obtained through a 65 μm stack of mouse cerebellum labeled with a combination of fluorescent proteins. In the online color version of this image one can see the unique colors produced and spectrally detected by the genetic combinations of individual fluorescent proteins which the authors label as XFP's. These colors were used to trace and map the various synaptic circuits. This figure was reproduced with permission from (Livet et al., 2007). This figure was originally published in color, and can be seen online in color, but has been altered for the print version of this article in black and white.

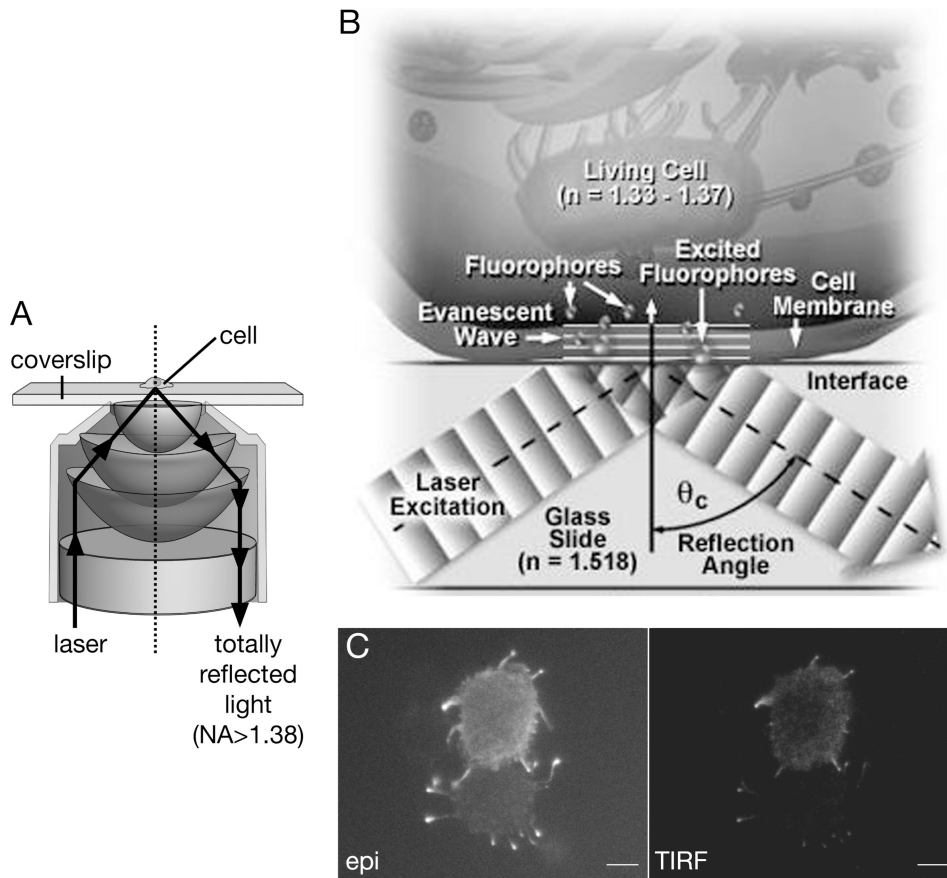


Figure 5. TIRF microscopy excites a shallow region above the coverslip using oblique laser excitation which is totally internally reflected and produces an evanescent wave for fluorophore excitation. **A. Internal reflection.** Light propagating through the periphery of a high numerical aperture objective (>1.38) is totally internally reflected by the coverslip and sent down the opposing side of the objective. **B. Evanescent wave is formed** when the critical angle θ_c is reached and the light is totally reflected. The reflection at the coverslip is due to the oblique angle of illumination and the mismatch of refractive index (n) between the oil and coverslip. Note that the evanescent wave only excites fluorophores where the cell attaches or is touching the coverslip. **C and D (no D indicated)** show a wide-field and TIRF image, respectively, of GFP tagged myosin V from *Drosophila* embryo hemocytes. Comparing the two images it is evident where the Myosin 5 is closest to the coverslip particularly in the bottom cell. Hemocytes courtesy of Amy Hong, NHLBI, NIH. Figure B was reproduced with permission from Mike Davidson (Florida State University and the National High Magnetic Field Laboratory) and the Molecular Expressions website.

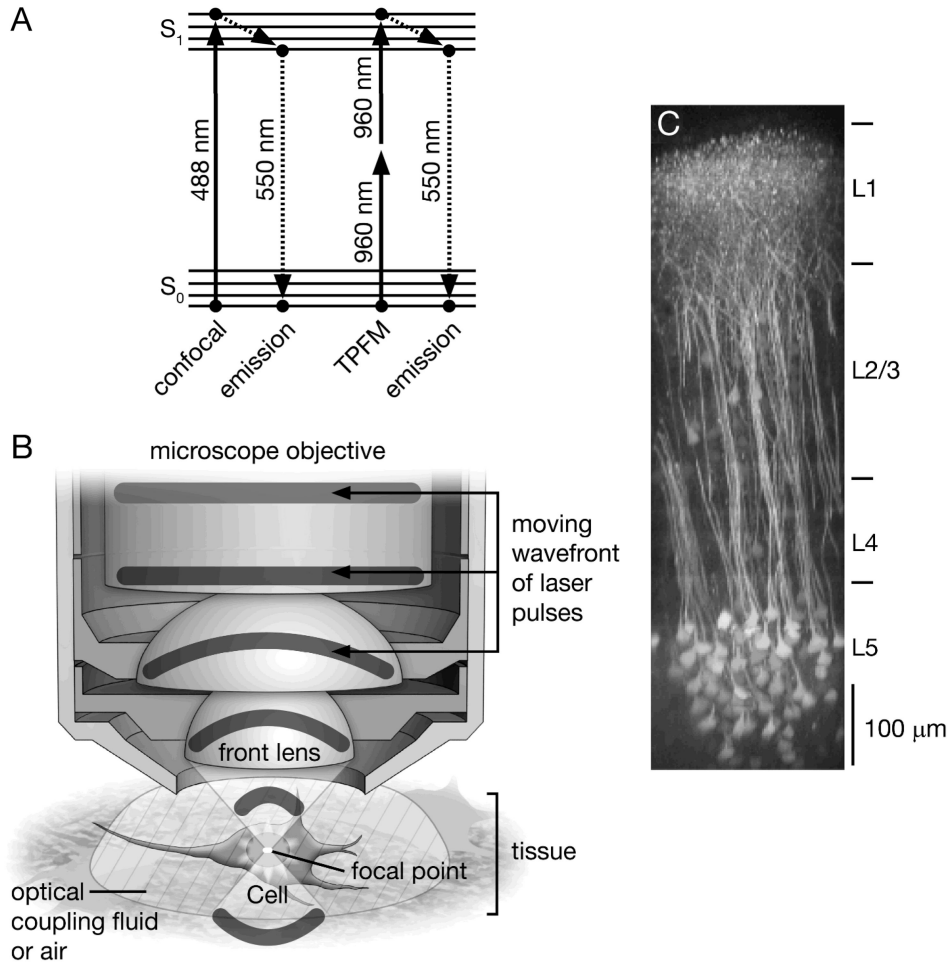


Figure 6.

Principals of two-photon fluorescence microscopy (TPFM). **A** shows a regular one-photon (e.g. confocal) and TPFM energy transitions in a Jablonski diagram. In TPFM two photons are absorbed nearly simultaneously to produce twice the energy. In this example GFP is excited with 960 nm light for TPFM and 488nm higher energy light for a confocal experiment. The emission is the same for both cases. It should be noted that TPFM absorption spectra for most fluorophores, including GFP, are very broad (in some cases hundreds of nanometers), and that the maximum is roughly a little less than twice the one-photon absorption maxima. **B** Two-photon fluorescence is generated in only one plane when a laser pulse train propagating through an objective is focused to a spot. Fluorescence is generated only at the point where the maximal photon crowding occurs and falls off from this plane at a rate of the fourth power from the center of the focal spot. **C** *In vivo* TPFM image of a mouse neocortex genetically labelled with a chloride indicator. This image shows the remarkable depth to which TPFM imaging is possible. Figure **C** is reproduced with permission from (Helmchen and Denk, 2005).

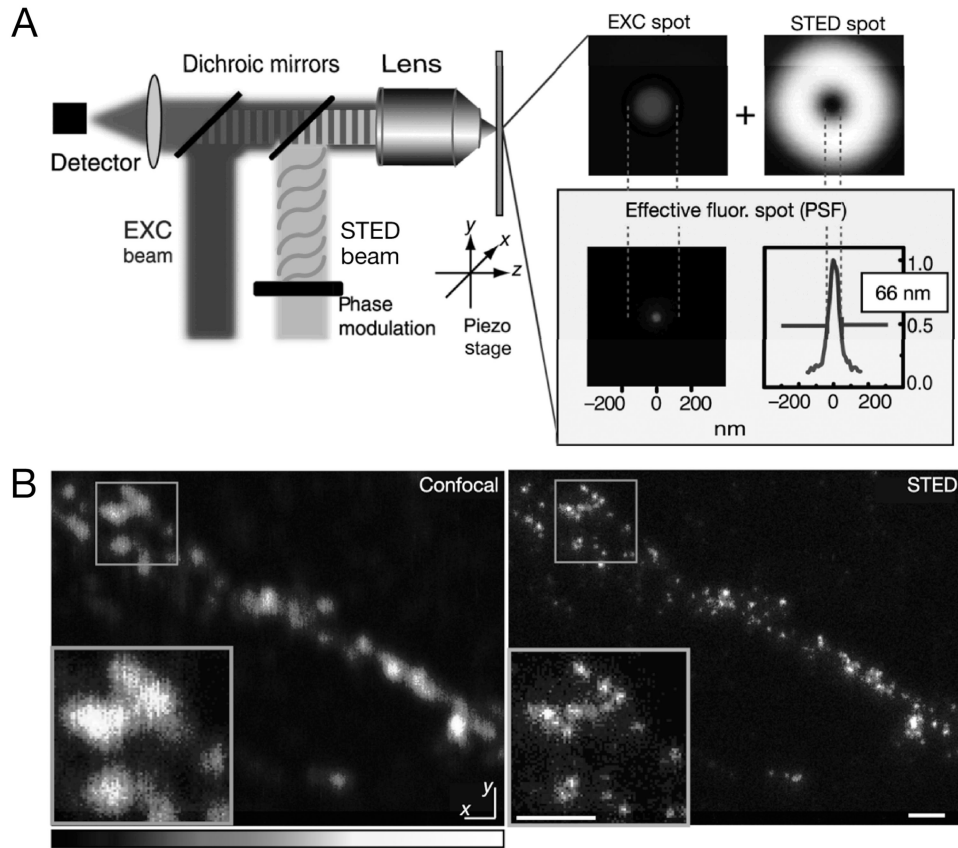


Figure 7. Technical principals of Stimulated Emission Depletion (STED) microscopy. **A.** The combination of the normal excitation beam with the phase modulated STED beam produces a sub-diffraction emission spot. The images on the right in (A) show the doughnut pattern produced by the phase modulation of the STED beam. This beam when overlapped with the diffraction-limited excitation spot quenches emission where the beams overlap leaving the middle, sub-diffraction sized, spot for spontaneous fluorescence. **B.** Comparison of confocal (left) and STED (right) images reveals a marked increase in resolution by STED since more labeled particles are visualized. Scale bar, 500 nm. Figure reproduced with permission from (Willig et al., 2006b).

Comparison of selected characteristics of commercially available microscope techniques discussed in this unit (Black boxes are best in category, grey are worst).

Table 1

Technique	Resolution XY	Resolution Z	Resolution Temporal	Imaging Depth	Ease of Use	Cost	Photobleaching or Phototoxicity
Wide-field	diffraction limited ($\approx 200\text{nm}$)	Weak	Best (ms/ Frame, signal limited)	Worst	simple	\$	Best (usually μWatts)
Structured Light	Varies (can be super-resolution)	Varies (can be super-resolution)	Varies based on number of images needed	Better	Varies with resolution needed	\$\$	Varies with number of images needed
Laser- Scanning Confocal (LSC)	Diffraction limited	Good ($>700\text{nm}$)	Typically slow (1s/frame)	Better (less than $100\mu\text{M}$)	Complex but most versatile	\$\$\$\$	Can be bad (μWatts of power focused to spot)
Multi-Point/Slit Confocal	Range to diffraction limit	Good same as LSC	Good (signal limited)	Better (same as LSC)	Better	\$\$\$	Better (usually lower flux density than LSM)
TIRF*	Diffraction limited but low background	Best but only first $200\text{-}300\text{nm}$	Good (signal limited)	$<300\text{nm}$	Good	\$\$	Better
Two-Photon (TPFM)	Diffraction limited	Good (slightly less than LSC)	Typically slow (1s/frame)	Best (hundreds of μMs)	Complex	\$\$\$\$\$	Can be bad (mWatts power focused to spot but limited to 1 plane)
STED**	Super-resolution ($<70\text{nm}$)	Same as TPFM	Slowest	???	Most complex	Very high cost	Worst (second beam with many mWatts of power)

* TIRF-Total Internal Reflection Fluorescence

** STED-Stimulated Emission Depletion